

GGNN: Graph-Based GPU Nearest Neighbor Search

Fabian Groh[✉], Lukas Ruppert[✉], Patrick Wieschollek, and Hendrik P. A. Lensch

Abstract—Approximate nearest neighbor (ANN) search in high dimensions is an integral part of several computer vision systems and gains importance in deep learning with explicit memory representations. Since PQT (Wieschollek *et al.*, 2016), FAISS (Johnson *et al.*, 2021), and SONG (Zhao *et al.*, 2020) started to leverage the massive parallelism offered by GPUs, GPU-based implementations are a crucial resource for today's state-of-the-art ANN methods. While most of these methods allow for faster queries, less emphasis is devoted to accelerating the construction of the underlying index structures. In this paper, we propose a novel GPU-friendly search structure based on nearest neighbor graphs and information propagation on graphs. Our method is designed to take advantage of GPU architectures to accelerate the hierarchical construction of the index structure and for performing the query. Empirical evaluation shows that GGNN significantly surpasses the state-of-the-art CPU- and GPU-based systems in terms of build-time, accuracy and search speed.

Index Terms—Nearest neighbor searches, graph and tree search strategies, information retrieval, approximate search, similarity search, big data

1 INTRODUCTION

APPROXIMATE nearest neighbor (ANN) search plays a crucial and long-standing role in various domains, including databases, computer vision, autonomous vehicles, personalized medicine, and machine learning. Since collecting large amounts of data became easier, the creation of a scalable and efficient data structure for retrieving similar items has become an active research topic. Despite all recent advances, the only available method for guaranteed retrieval of the exact nearest neighbor in high dimensions is still exhaustive search, due to the curse of dimensionality [4]. Even when leveraging modern hardware, it remains impractical to perform an exhaustive search over billions of high-dimensional data points. Instead, most popular methods relax the problem by searching for an entry that is likely to be the nearest neighbor, accepting a minimal loss in accuracy.

Besides designing a very fast GPU-based approximate kNN query algorithm, we address the efficient construction of a hierarchical graph-based search structure. Building time becomes more and more important in dynamically growing or changing datasets for on-the-fly analysis, e.g., in correspondence and feature matching for tracking and

object recognition in videos, for newly embedded vectors of neural networks similar to DEEP1B [5], or in recommender systems [6]. Our graph-construction explicitly determines the true k nearest neighbors of each point in the dataset with high probability. Solving this for-all task is highly relevant in n -body problems like salient point estimation, kernel-density computation, cluster analysis, retrieval of more robust prototypes, or feature matching in embeddings.

To keep up with the scale of data that is produced day by day, modern approaches use index structures that are heavily tailored towards exploiting the massive parallelism of GPUs [1], [2], [7], [8] or custom hardware [9], as opposed to previous CPU-based methods [10], [11], [12], [13], [14], [15], [16], [17].

The quality of the recall heavily depends both on the choice of the search structure and the executed search (query) itself. Structures based on quantization or hashing/binning schemes [1], [2], [11], [12], [13], [14], [15], [16], [17], [18], [19] can be built efficiently, but typically suffer from relatively low recall rates as enumerating and visiting neighboring cells is exhaustive in high dimensions. Better recall rates are recently achieved by graph-based methods [8], [20], [21], [22], [23], [24], [25], [26], [27]. Existing methods for constructing effective search-graphs, e.g., [20], update varying-sized edge lists sequentially. They are highly dependent on global memory synchronization and difficult to parallelize effectively beyond a few cores. Hence, their construction times are not scaling well and are measured in hours or even days [19], [27].

Given a precomputed graph structure, a query traverses the edges of the graph to decrease the distance to a query point. It needs to compute the distances to all neighbors of the currently investigated node, move to the next-best point and store which points have already been visited. All decisions are made locally and independent for each query, rendering the query algorithm an ideal candidate for parallelization.

- Fabian Groh and Patrick Wieschollek are with Amazon Tübingen, 72076 Tübingen, Germany. E-mail: fabian.groh@gmail.com, mail@patwie.com.
- Lukas Ruppert and Hendrik P. A. Lensch are with Computer Graphics Group, University of Tübingen, 72074 Tübingen, Germany. E-mail: {lukas.ruppert, hendrik.lensch}@uni-tuebingen.de.

Manuscript received 7 Mar. 2021; revised 8 Mar. 2022; accepted 11 Mar. 2022. Date of publication 22 Mar. 2022; date of current version 16 Jan. 2023.

This work was supported by the Deutsche Forschungsgemeinschaft (DFG, German Research Foundation) under Germany's Excellence Strategy – EXC number 2064/1 under Grants 390727645 and SFB 1233, TP 02 under Grant 276693517 and also supported by the German Federal Ministry of Education and Research (BMBF): Tübingen AI Center, FKZ: 01IS18039A.

(Corresponding author: Fabian Groh.)

Recommended for acceptance by H. Kitagawa.

Digital Object Identifier no. 10.1109/TBDATA.2022.3161156

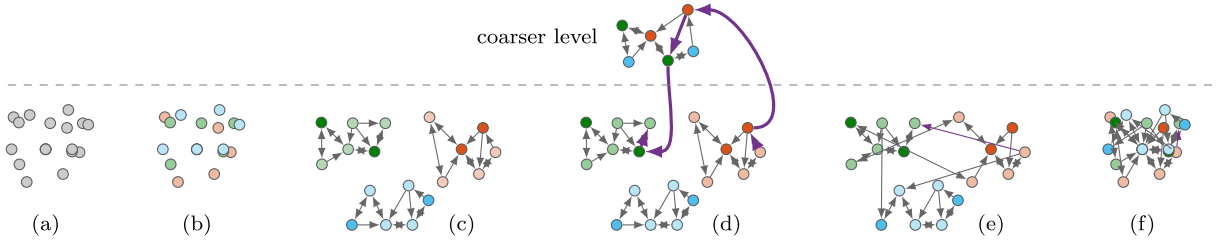


Fig. 1. Illustration of the bottom-up construction of the kNN-graph for a dataset (a). After random partitioning (b), a kNN-graph is constructed for each partition (c). A selection of nodes builds a coarser kNN-graph (d), which is used to propagate links between partitions. These links are used to merge several partitions (e) into a final kNN-graph (f).

However, a parallel implementation needs to carefully address a number of issues to be efficient. For one, the available memory bandwidth for loading each vector to compare with might become a limiting factor. Here, Optane memory [27] or GPUs [3] offer a solution. Second, on GPUs one needs to cope with the limited amount of available per-thread or per-block memory when storing the list of visited points.

Hence, we propose a GPU-friendly query design on thread-block level with high on-chip resource utilization through a fully parallel multi-purpose cache and a fixed number of neighbors per point. Further, we introduce a novel technique for very fast graph construction that utilizes the fast parallel query algorithm to iteratively merge multiple sub-graphs together. This bottom-up construction scheme is sketched in Fig. 1. Hierarchical graphs are used as a global optimization substitution to overcome gaps in local connectivity, in particular during construction. Additionally, our local symmetric linking approach reduces the amount of redundant links in the graph to circumvent negative impacts of overflows in the memory-limited caches.

Our approach is also inherently suited for batch processing by already generating multiple sub-graphs at the same time. By forgoing the final merge of several sub-graphs into one combined graph, one can easily obtain independent yet effective sub-graphs for parts of large-scale datasets which would otherwise not fit in memory. These can easily be processed even on multiple GPUs at the same time where each query then needs to be executed once on each shard. This simple yet effective method allows for optimal multi GPU utilization.

To summarize our main contributions, we propose a method for extremely fast approximate kNN-search on GPUs for high-dimensional data. We focus not only on fast query time, but also on a very efficient construction of the index structure, while still achieving high recall rates of the true nearest neighbours.

As evidenced by our empirical evaluation, the presented scheme outperforms existing approaches concerning both the construction as well as the query time. At the same time, the recall rate is consistently high and can be traded in for even faster construction or query time. We present a multi-GPU scheme that is capable of achieving above 99% recall even for common benchmark datasets with billions of high-dimensional entries.

2 RELATED WORK

A large amount of literature exists on designing structures that accelerate a nearest neighbor search. Besides traditional

approaches [10], [28], most popular techniques rely either on data quantization in clusters [1], [2], [11], [12], [13], [14], [15], [16], [17], [18], [19] or building neighborhood graphs [8], [22], [23], [24], [25], [26], [27]. To achieve peak performance, most of these methods compute a compressed representation for each entry as large datasets will not fit into fast memory. There exist several strategies to compute such a compression. While hashing methods [29], [30], [31] produce compact binary codes, quantization-based methods reuse centroids by assigning each data point a unique identifier based on the centroid to which they belong. It has been empirically shown that quantization methods are more accurate than various hashing methods [10], [11].

Quantization methods for nearest neighbor search using clustering methods were popularized by Jégou *et al.* [11] while originally being introduced in [32]. Such index structures, like IVFADC [11], partition the high-dimensional search space into disjoint Voronoi cells described by a set of centroids obtained by Vector Quantization (VQ) [33]. The idea has been extended later by Babenko *et al.* [15], where the high-dimensional vector-space is factored in orthogonal subspaces. Hereby, each vector is assigned to a centroid independently for each subspace according to a separate codebook that resides there. Wieschollek *et al.* [1] proposed a hierarchical representation of the codebook besides demonstrating superior performance using a GPU. Johnson *et al.* [2] ported IVFADC [11] to the GPU in combination with a fast GPU-based implementation for k -selection, i.e., returning the k lowest-valued elements from a given list (a crucial part of quantization based methods). They are the first employing multi-GPU parallelism by replication and sharding. Their work forms the library “FAISS”. Eventually, Chen *et al.* [18] proposed a GPU based method RobustIQ overcoming the memory limitations of FAISS by extending the idea of Line Quantization from [1] in a hierarchical fashion. Still, the reported distances are only an approximation of the true distance.

All hashing and quantization-based indexing schemes share the same problem that they partition the space into cells. While the containing cell for a query might be found very efficiently, the exact nearest neighbor might be across the boundary to one of the neighboring cells. Determining and visiting all neighboring cells in high dimension is a problem severely limiting these approaches.

kNN-graph based methods are another way to accelerate the query process. Our presented approach belongs to this category. The main idea is to link each point from the search space to k of its nearby points. Each query will start at a random guess in the dataset. Then, the guess itself is refined by

replacing it with a better point from the k linked neighbor points. Chen *et al.* [23] propose a fast divide and conquer strategy for computing such kNN-graphs. Done *et al.* [22] introduced NN-descent for using kNN-graphs to accelerate NN-search. Hereby, each point maintains a list of its own nearest neighbors and points where itself is considered as a nearest neighbor. This has been later extended [24] to make use of MapReduce. EFANNA as a multiple hierarchical index structure uses a truncated KD-tree to build a kNN-graph [25].

In the ideal case, a kNN-graph augmented with additional links could guarantee that for an arbitrary starting point the NN-descent will converge to the correct solution. Computing such a graph with additional links at scale is not practicable. Therefore, several methods exist to at least approximate such a graph [8], [26]. Fu *et al.* [26] introduce NSG as an approximation. To reduce the overall number of edges, their optimization tries to lower the out-degree individually per node. Their method can scale beyond multiple cores, outperforming a GPU approach [2] on a benchmark dataset. Harwood *et al.* [8] suggest an alternative approach for constructing such a graph. Starting from a fairly dense graph, they remove “shadowed edges”, which are redundant when considering traversing paths during a query. They showed promising results using the GPU but only on rather small datasets as their build time is rather high. Mal'kov *et al.* [20] construct a hierarchical graph structure to accelerate the nearest neighbor search.

For graph-based methods, memory throughput is often the limiting factor. Ren *et al.* [27] propose an optimized construction of HNSW-style search graphs on out-of-core datasets using heterogeneous memory. Using fast Optane memory allows them to quickly query even billion-scale datasets at high accuracy. Zhao *et al.* [3] propose GPU-based “search on graph” (SONG) using index structures built using either HNSW [20] or NSG [26], achieving significant speedup over CPU-based queries in most cases.

Our method is most similar to HNSW [20] with its hierarchical construction, but it is very carefully tuned for optimal parallelism of construction tasks and also differs during the query.

3 BACKGROUND

In this section, we formally introduce the approximate nearest neighbor (ANN) problem statement and used notation.

3.1 Nearest Neighbor Search

The nearest neighbor problem retrieves a point x^* from a dataset $\mathcal{X} = \{x_1, \dots, x_n\}$ that has the smallest distance to a query q . For the sake of simplicity, here, we assume an euclidean space ($\mathcal{X} \subset \mathbb{R}^d, q \in \mathbb{R}^d$) and euclidean distances ($\|\cdot\|_2$). The nearest neighbor $x^* \in \mathcal{X}$ of q therefore is defined as

$$x^* = \arg \min_{x \in \mathcal{X}} \|q - x\|_2. \quad (1)$$

Similarly, the k -nearest neighbor search retrieves the k closest entries from \mathcal{X} for a given query. As finding the exact nearest neighbor might be costly, we may accept points in \mathcal{X} which are close to q and therefore deliver an approximate solution to Eq. (1).

3.2 KNN Graph

In a kNN-graph, each point x from the dataset \mathcal{X} represents one node in the graph G . Further, we define $\mathcal{N}_x \subseteq \mathcal{X}$ as a local neighborhood of x with k elements and defer the details on how to construct \mathcal{N}_x to the next section. The edges E of the graph are then defined as (x, y) where $y \in \mathcal{N}_x$. Note that the resulting graph is a directed graph $G = (\mathcal{X}, E)$, where $E = \{(x, y) \mid x \in \mathcal{X}, y \in \mathcal{N}_x\}$ and $(x, y) \in E \Rightarrow (y, x) \in E$.

One greedy algorithm to find the nearest neighbor for a query point q is *NN-descent* [22]. Starting from an initial guess $x \in \mathcal{X}$, the distance between q and each neighboring point $y \in \mathcal{N}_x$ is computed. If any $y \in \mathcal{N}_x$ is closer to q than x , the guess x is replaced by the closest point from \mathcal{N}_x to q . This process iterates until no point in \mathcal{N}_x has a smaller distance to q than x . However, as the current x might not provide an edge into the right search direction, this greedy algorithm might get stuck in a local minimum on a pure kNN-graph.

3.2.1 Common Pitfalls

Since the NN-descent is a greedy search, it offers no guarantee on finding the exact solution. Some of the reasons are listed below:

Connectivity: As a kNN-graph is a directed graph, y might be directly connected to x , being its nearest neighbor, hence $y \in \mathcal{N}_x$. But this does not imply that the inverse link exists ($y \in \mathcal{N}_x \not\Rightarrow x \in \mathcal{N}_y$). Therefore, the construction of an augmented (diversified) kNN search-graph has to deal with synchronizing outgoing and incoming (inverse) **edges**.

Gaps in high-dimensional spaces: As each point is only linked to a finite number of local neighbors, there exist pathological cases (even in 2D), where close-by points are not directly connected at all. Such a case is illustrated in Fig. 3. Due to the gap, the true nearest neighbor will not be found. Computing an idealized monotonic relative neighborhood graph [26] (MRNG) would avoid this issue, but requires a strongly varying connectivity not suitable for parallel approaches – besides its additional computational **burden**.

Degree of nodes: There exists a trade-off when choosing the cardinality of \mathcal{N}_x for any $x \in \mathcal{X}$. Having fewer edges amplifies the previously described issues, but also reduces the number of necessary comparisons at each step. Conversely, having many edges allows the greedy search to escape from local neighborhoods but increases the cost for each iteration.

4 GPU-BASED NEAREST NEIGHBOR SEARCH

Searching for the k nearest neighbors for multiple queries, given some graph structure, is the central operation for various applications and also the main building block for our graph construction (see Section 5). Achieving high recall rates at very short times is the primary goal of our parallel GPU-based search-algorithm on kNN-graph structures. The algorithm can, within bounds, be tuned for quality or speed, offering a solution to a broad range of use-cases, accommodating those requiring high recall rates as well as real-time algorithms with reduced quality constraints.

The main idea is to highly parallelize the search by utilizing one thread-block per query. In contrast to the naïve

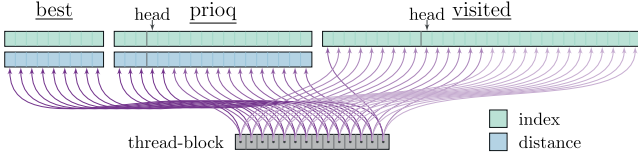


Fig. 2. Our cache consists of a *best* list, *prioq* (priority queue) and a *visited* list. It resides entirely within shared memory. The *best* list and *prioq* both contain indices and distances and are sorted by distance. The *visited* list contains only indices to preserve memory. The *prioq* and the *visited* list are implemented as ring buffers. This allows elements to be easily popped from the front of the *prioq* and to overwrite old elements in the *visited* list once it is full. The cache is accessed and maintained in parallel by the entire thread-block.

solution of a query per thread, the main advantage is to bundle enough on-chip resources that all meta-data can be kept on very fast memory. This is of utmost importance, since graph-based methods still need to load a large amount of neighborhood information as well as vectors from global memory for distance computations. In addition, the thread-block approach guarantees high memory bandwidth through very efficient coalesced memory accesses. It also allows to perform more computation in parallel since common tasks like distance computations or the maintenance of priority queues and visited lists can be parallelized. Furthermore, individual queries that vary in runtime can be scheduled independently.

4.1 GPU-Based Search With Backtracking

Assuming a diversified (see Section 5.2) kNN-graph with given starting points $s \subset \mathcal{X}$, for a query $q \in \mathbb{R}^d$, the simple greedy downhill search with backtracking from Algorithm 1 is executed. First, the cache structure (see Section 4.1.1) is initialized (*init*) with the query point and a slack factor τ (see Section 4.1.2). Then, the starting points s are introduced to the cache by *fetch*, which computes their distances to the query q and adds them to the priority queue (*prioq*). As starting points s , we use the nodes on the top-layer of our hierarchical graph (see Section 5.4).

Until there are no more unexplored points in the priority queue, all neighbors \mathcal{N}_a of the closest not yet visited point a are being fetched to the cache. Essentially, performing a depth-first search in the graph. Our cache structure manages a sorted list of the k closest points (*best*) to the query which are observed during the traversal. Hence, the *best* list is returned as the result of the search.

4.1.1 Caching on GPUs

The centerpiece of our fast GPU-based kNN search is a multi-purpose cache (see Algorithms 1 and 2). One of the major deficits of GPUs is their limited on-chip memory (*register* and *shared memory*¹) that can be accessed with low latency.

In particular, kNN-graph algorithms have a strong demand for highly dynamic structures like unpredictably growing lists of potential points to visit or of already visited points. These meta-data are perused and modified frequently during the query.

The cache's memory layout is shown in Fig. 2. It consists of three major parts:

- 1) *best*: A sorted list of the points closest to the query and their distances.
- 2) *prioq*: A priority-queue that manages points to be visited as a distance-sorted ring-buffer.
- 3) *visited*: A ring-buffer that caches indices of already visited points in a first in first out (FIFO) fashion.

All three parts are handled in *shared memory*. The combined length is a multiple of the assigned threads, hence, every thread has multiple work items.

Algorithm 1. Basic Query With Backtracking

Function query(G, s, q, τ, k):

Input: search-graph G with start points s , query point q , slack factor τ (see Section 4.1.2)

Output: k closest points to q

cache.init(q, τ) /* (see Section 4.1.1) */

cache.fetch(s)

while ($a \leftarrow \text{cache.pop}()$) $\neq \emptyset$:

cache.fetch(\mathcal{N}_a) /* (see Section 3.2) */

return *cache.best*

The main methods of our cache are shown in Algorithm 2 and described in the following paragraphs. Note that for ease of readability synchronization barriers preventing race conditions are omitted. We refer to our published open source code² for more information. For the purpose of visualization, *shared memory* variables are denoted with an underline, while normal variables can be assumed to live in *register space*.

Fetch. Given a list of point proposals p , first, known elements are removed from the proposal list. Each proposal is compared in parallel against the working items of each thread and removed in case of a match. The remaining proposals are processed iteratively. The distance to the query point is computed in parallel (*dist*). Every thread reads its respective vector element(s) from memory and computes the element-wise result. A subsequent reduction produces the complete distance. For parallel primitives like reduction, we use NVIDIA's CUB³ library for highly optimized implementations. The parallel coalesced loading and processing is highly effective in terms of GPU utilization. Points that are inside our criteria are pushed to the cache structure.

Push. For a given pair of index p and distance d , the *push* method performs a parallel insertion into the distance-sorted lists of *best* and *prioq*. To perform the insertion, all items with index c_i that have a distance which is greater than d are temporarily copied into the thread-block's registers and are written back into the subsequent index c_{i+1} unless the end of the list or ring-buffer is reached. The new element is inserted where the item to the left is closer than the new item, or at the beginning if the new item is closer than all previous items. Consequently, a point that is eligible for *best* and *prioq* will be inserted in both lists simultaneously.

1. <https://docs.nvidia.com/cuda/>

2. <https://github.com/cgtuebingen/ggmn>

3. <https://nvlabs.github.io/cub/>

Since *prioq* is a ring-buffer, the logical beginning and end positions are dependent on the head position. Hence, index computations on the physical borders need to be wrapped around.

Pop. This single-threaded routine returns the current head of the priority queue and manages the ring-buffers. Our criteria is monotonically decreasing over the course of a query (inspect Section 4.1.2). Hence, if the head of the *prioq* violates the criteria, we are able to safely terminate the query. In the valid case, the point is removed from the *prioq* and added to the *visited* list at the head position. Both head pointers are moved one step forward. Finally, the point is returned.

Algorithm 2. Cache Operations

```

Function fetch(p):
  Input: Point proposals p.
  parfor  $p_{c_i} \in \{\text{best}, \text{prioq}, \text{visited}\}$ :
    for  $p \in \underline{p}$ :
      if  $p_{c_i} = p$ :
        remove  $p$  from p
    for  $p \in \underline{p}$ :
       $d \leftarrow \text{dist}(p)$  /* Compute in parallel. */
      if  $\text{criteria}(d)$ :
        push( $p, d$ )
Function push( $p, d$ ): /* Parallel insertion */
  Input: Point proposal  $p$  with distance  $d$ .
  parfor  $p_{c_i}, d_{c_i} \in \{\text{best}, \text{prioq}\}$ :
    /* Read  $p_{c_i}$  and  $d_{c_i}$  and sync. */
    if  $d_{c_i} \geq d$ :
      if  $\text{is\_not\_end}(c_i)$ :
         $\underline{p_{c_{i+1}}} \leftarrow p_{c_i}$ 
         $\underline{d_{c_{i+1}}} \leftarrow d_{c_i}$ 
      if  $\text{is\_begin}(c_i)$  or  $\underline{d_{c_{i-1}}} < d$ :
         $p_{c_i} \leftarrow p$ 
         $d_{c_i} \leftarrow d$ 
Function pop(): /* Single-threaded routine */
  Output: Returns head of priority queue.
   $p, d \leftarrow \underline{\text{prioq\_head}}$ 
  if not  $\text{criteria}(d)$ :
    return empty
  /* Remove point from prioq. */
   $\underline{\text{prioq\_head}} \leftarrow \text{empty}$ 
  move_head_forward( $\text{head}_{\text{prioq}}$ )
  /* Add point to visited list. */
   $\underline{\text{visited\_head}} \leftarrow p$ 
  move_head_forward( $\text{visited\_head}$ )
  return  $p$ 
Function criteria( $d$ ):
  return  $d \leq d_{\text{best}_k} + \xi$  /* (see Section 4.1.2) */

```

4.1.2 Stopping Criterion

On high-dimensional data, algorithms that solely rely on greedy downhill search will quickly get stuck in local minima. On the other hand, complete backtracking might visit the entire dataset.

A common stopping criterion, e.g., [20], is to terminate the search once the *best* list cannot be improved by adding the closest not yet visited element, i.e., once $d > d_{\text{best}_K}$.

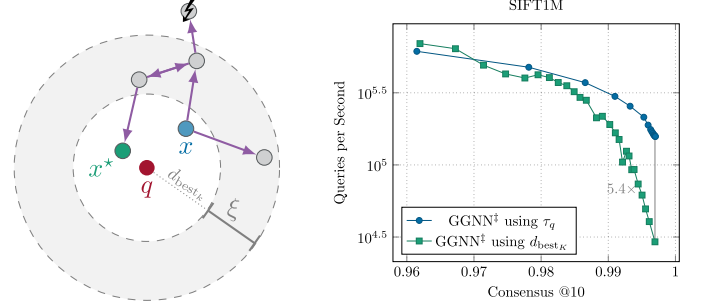


Fig. 3. Allowing a slack ξ makes it possible to escape a local minimum $x \in \mathcal{X}$, eventually reaching the solution $x^* \in \mathcal{X}$ for a given query $q \in \mathbb{R}^d$. Points outside of this boundary are unlikely to provide helpful links and are discarded to reduce computational cost. (right) Comparison of using our stopping criterion (τ_q) to using a growing *best* list to terminate queries. With the *best* list based approach, high recalls can only be achieved in conjunction with high memory usage which slows down the query.

where d is the distance of the new element and d_{best_K} is the distance of the last element in the *best* list. To achieve higher recalls, the *best* list needs to be extended (K needs to be increased), potentially by hundreds of elements.

We propose an efficient approximation by adding an adaptive, monotonically decreasing slack ξ to the distance of the k -closest neighbor: $d_{\text{best}_K} \approx d_{\text{best}_k} + \xi$, where $k \ll K$, that allows us to limit the size of the *best* list to only the k closest neighbors which are to be queried (or at least 10). Instead of explicitly tracking the distance of further neighbors, the slack accounts for a safety margin to ensure that the path to the closest neighbor will likely be found, e.g., Fig. 3. The search will terminate once

$$d > d_{\text{best}_k} + \xi, \quad \xi = \tau \cdot \min\{d_{\text{best}_1}, d_{\text{nn}_1}^+\}. \quad (2)$$

The slack factor τ controls the size of the safety margin. d_{best_1} is query-specific and relates the margin to the currently best found match while $d_{\text{nn}_1}^+$ correlates with the density of the given database nodes. Specifically, $d_{\text{nn}_1}^+$ provides a global limit (to catch outliers) that is calculated during graph construction. It denotes the maximum distance to the closest neighbor across all points within the currently processed subset of the graph \mathcal{S}

$$d_{\text{nn}_1}^+ = \max_{x \in \mathcal{S}} \left\{ \min_{y \in \mathcal{N}_x} \|x - y\|_2 \right\}, \text{ where } \mathcal{S} \subseteq \mathcal{X}. \quad (3)$$

Using our stopping criterion keeps the *best* list at a small size and by that reduces the amount of shared memory required for performing the query. As demonstrated by Fig. 3, our stopping criterion allows for high efficiency even at high accuracy.

Typical values for τ are above 0 and below 2. Larger values improve accuracy with diminishing returns.

5 APPROXIMATE SYMMETRIC NEAREST NEIGHBOR GRAPH CONSTRUCTION

The construction of proper CPU-based kNN search-graphs is performed typically in a sequential procedure on global graphs. Edges are either attached (e.g., [20]), or pruned (e.g., [8], [21], [26]) one after the other. During the process, Authorized licensed use limited to: Xian Jiaotong University. Downloaded on October 20, 2024 at 14:04:37 UTC from IEEE Xplore. Restrictions apply.

the edge-lists per node tend to vary heavily ranging from completely empty to complete lists of all possible points. While these global optimization approaches are able to produce high quality graph structures on CPUs, for fast GPU-based construction, they are impractical.

We propose a parallel graph construction based on parallel merging of hierarchical kNN search-graphs as sketched in Fig. 1. By partitioning the task of constructing the search graph into small, parallelizable tasks, we are able to efficiently use the massive parallelism offered by GPUs. In the following, we present our parallel graph construction process, followed by details on the hierarchical query process, and the graph-diversification and refinement by symmetric linking. Finally, we look at how to best perform the final queries and multi-GPU configurations.

5.1 Building the Hierarchical kNN-Graph

Our construction process (Algorithm 3) builds the kNN search-graph bottom-up by recursively merging smaller search-graphs.

Algorithm 3. Parallel Graph Construction

```

Function BuildGraph( $\mathcal{X}, L, k, \tau_{build}$ ):
  Input: Dataset  $\mathcal{X}$ , number of layers  $L$ , number of neighbors
           per point  $k$ , slack factor  $\tau_{build}$ 
  Result: search structure graph
  graph  $\leftarrow$  init( $\mathcal{X}, L, k, \tau_{build}$ )
  for  $l_{top} \leftarrow 0$  to  $L - 1$ :
    if  $l_{top} > 0$ :
      graph.select( $l_{top}$ )
    for  $l_m \leftarrow l_{top}$  to  $0$ :
      graph.merge( $l_{top}, l_m$ )
      graph.sym( $l_m$ )
  Function graph.merge( $l_{top}, l_m$ ):
    parfor  $z \in$  graph.layer( $l_m$ ):
      /* Use brute force if  $l_{top} = l_m$ . */
       $b_z \leftarrow$  graph.query( $z, l_{top}, l_m$ )
  graph.layer( $l_m$ )  $\leftarrow b$ 
  if  $l_m = 0$ :
    graph.stats()
  Function graph.sym( $l_i$ ):
    parfor  $z \in$  graph.layer( $l_i$ ):
      graph.sym_links( $z$ )

```

To initialize the process, we logically partition the entire dataset \mathcal{X} into small batches of size s , e.g., 32. These represent hierarchical search-graphs of height 1. We initialize the neighbors within the bottom layer by first performing the mergeoperation which initializes the k outgoing edges per point with each point's nearest neighbors. Then, the symoperation replaces up to k_{sym} outgoing links in an effort to approximate an undirected graph, details in Section 5.2.

In order to merge the individual sub-graphs, we first select s points from the groups of g graphs which each are to be merged. These selected points now form batches representing the new top layer. There, we perform the same operations as with the bottom-layer before. We merge, i.e., query for the nearest neighbors to fill the outgoing edge list and perform graph-diversification (sym). As the nearest neighbor of any point might be found in any sub-graph, edges across batch boundaries will be introduced. **These**

steps now repeat top-down until the entire hierarchical search-graph is interconnected.

Whenever the bottom layer is reached, we also save the distance to the first nearest neighbor d_{nn1} for each point and compute the mean and max over the dataset (stats). This allows for an easy adaption of our stopping criterion to every dataset without any precomputation. Initially, the maximum is prone to outliers in the still coarse nearest neighbor graph. Therefore, during construction, we substitute the maximum distance to the closest neighbor d_{nn1}^+ in Eq. (2) with the mean distance \bar{d}_{nn1}

$$\bar{d}_{nn1} = \frac{1}{|\mathcal{S}|} \sum_{x \in \mathcal{S}} \left\{ \min_{y \in \mathcal{N}_x} \|x - y\|_2 \right\}, \text{ where } \mathcal{S} \subseteq \mathcal{X}. \quad (4)$$

For selecting the points for the top layer, weighted reservoir sampling with d_{nn1} as weights is used with the method of [34].

Algorithm 4. Hierarchical Query

```

Function graph.query( $z, l_{top}, l_m$ ):
  Input: query point  $z$  from layer  $l_m$ , start layer  $l_{top}$ , and end
           layer  $l_m$ 
  Output:  $k$  closest points to  $z$ 
  cache.init( $z, \tau$ )
   $s \leftarrow$  getTopSegment( $z, l_{top}$ )
  cache.fetch( $s$ )
  for  $l_i \leftarrow l_{top} - 1$  to  $l_m$ :
    cache.transform( $l_i$ )
    while ( $a \leftarrow$  cache.pop())  $\neq \emptyset$ :
      cache.fetch( $\mathcal{N}_a$ )
  return cache.best

```

As all construction tasks can be performed in parallel for each point in each layer while requiring small, limited amounts of memory each, the construction can be performed quite quickly when exploiting the massive parallelism offered by GPUs.

Hierarchical kNN Graph Query. In a top layer, the mergeoperation can simply perform brute-force search between the s points per batch. With each lower layer, the number of batches grows with the factor g . To perform efficient searches for nearest neighbors in lower layers we perform a hierarchical query (Algorithm 4), which layer by layer utilizes the already merged upper layer to find entry points into the batches on the lower layers, and otherwise behaves just like the previously presented simple query (Section 4.1). The indices of the closest points found on the upper layer are then transformed into the indices of the same points on the next lower layer and the search continues until the target layer l_m is reached. While distances to already visited points can be reused, their neighborhood on the lower layers changes. Therefore, we allow all points to be visited again after switching between layers.

As in HNSW [20], the hierarchy allows us to bridge gaps in the connectivity as multiple entry points from the top layer may approach the query on the bottom layer from different sides.

5.2 Graph Diversification

In order to reach any point from any direction, every edge of the graph, in principle, should be undirected. However, when every point should at least know its k_{nn} nearest neighbors, the total number of edges per point x would vary significantly for an undirected graph as the number of points which have x as their nearest neighbor will heavily depend on the local **geometry**.

In order to obtain a regular representation and to allow for simple parallelized traversal with constant workload per step, our graph only consists of exactly k directed (i.e., outgoing) edges. We logically split the outgoing edges into at least $k_{nn} = k/2$ true nearest neighbors and up to $k_{sym} = k/2$ inverse links that are used to approximate an undirected graph.

As the number of representable inverse links is limited, one has to determine which of the inverse links are necessary. Harwood and Drummond [8] introduce the concept of shadowed links which are made redundant by the query's greedy exploration strategy. Optimizing the entire graph to remove all potentially shadowed edges requires a complex global optimization. The same holds for the construction of monotonic relative neighborhood graphs [26].

Our approach to graph diversification is to explicitly search for missing inverse links by querying for each point z from all its k_{nn} nearest neighbors $x_i \in \mathcal{N}_z^{nn}$ within a small search radius. Where a direct inverse link from x_i back to z exists, the query can trivially be skipped. When there is no path within the allowed range, the link is added (e.g., Fig. 4). The searches are executed in parallel over all points $z \in \mathcal{X}$, allowing for faster construction.

Algorithm 5. Symmetric Linking Query

```

Function graph.sym_links( $z$ ):
  Input: symmetric query point  $z$ 
  for each  $x_i \in \mathcal{N}_z^{nn}$ 
    cache.init( $z, \tau$ )
    cache.fetch( $x_i$ )
    while ( $a \leftarrow \text{cache.pop}()$ )  $\neq \emptyset$ :
       $p \leftarrow \mathcal{N}_a^{nn} \cup \mathcal{N}_a^{sym}$ 
      if  $z \in p$ :
        skip  $x_i$ 
      cache.fetch( $p$ )
    for each  $p \in \text{cache.best}$ :
      if  $|\mathcal{N}_p^{sym}| < k_{sym}$ :
         $\mathcal{N}_p^{sym} \leftarrow \mathcal{N}_p^{sym} \cup \{z\}$ 
      break

```

The detailed symmetric linking operation is shown in Algorithm 5. Each point z launches queries for itself, starting from its k_{nn} nearest neighbors x_i . During the query, only the k_{nn} nearest neighbors of each visited point $\mathcal{N}_{x_i}^{nn}$ and potential already inserted symmetric/inverse links at that point $\mathcal{N}_{x_i}^{sym}$ are considered by the query as all others may still be overwritten. If a path back to z is found, the search continues with z 's next neighbor. Otherwise, a link to z is inserted at the closest point to z encountered during the search which still has free capacities in its inverse link list.

To avoid race conditions on the insertions, we use atomics to keep track of the inverse link list sizes. On

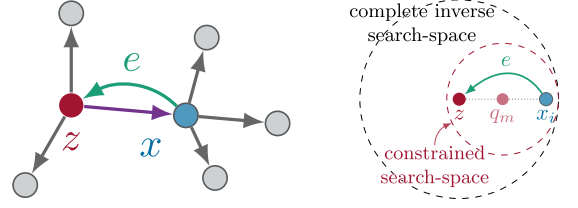


Fig. 4. Maintaining symmetric links. If there is no easily found connection from $x \in \mathcal{N}_z^{nn}$ back to $z \in \mathcal{X}$, the edge e is added to allow propagating nearest neighbor information between z and x . (right) Instead of considering the full search radius when probing whether to insert symmetric links, we constrain the maximum distance of points to be visited to the smaller sphere centered around the midpoint q_m .

average, less than $k/4$ inverse links are necessary this way. If no candidate is found, the link is ignored. In our setting, this is, however, a very rare case and z might potentially still be reachable through either through hierarchy or multiple start points.

5.2.1 Additional Symmetric Linking Constraint

As demonstrated in Fig. 4, the usual search-space would be defined depending on z and x_i . However, in order to generate a search structure that is able to find a path for all potential query points, we additionally constrain it on the worst-case query that still needs to find a path to z . Hence, a link is required to bridge the gap for a worst-case query on the midpoint q_m . Note, a path to x_i is given since it is directly known from z . For symmetric linking, only this search space is relevant, which is the circle defined by the center q_m and distance to x_i , but still encloses z . In practice, we set $q_m = z + 0.4 \cdot (x_i - z)$. This is slightly less conservative, but decreases the number of necessary symmetric links.

5.3 Graph Refinement

The initial graph construction might not always produce perfect results at the first trial. The reason for this is to some extent the large merge factor g that results when constructing search-graphs of low height that need to span over massive datasets.

In our experiments we found using a height of $L = 4$ for the hierarchical search-graph to provide the best performance. To create a single graph from the initially n/s disjoint sub-graphs consisting of single batches of size s (usually, $s = 32$), we need to merge groups of $g = \sqrt[L]{n/s}$ sub-graphs on each layer, where each new sub-graph's top-layer contains s points sampled from these g sub-graphs (see Section 5.1). While for $n = 256$, just 2 graphs need to be merged together each, for $n = 10^6$, about 32 graphs each need to be merged per layer. The higher g , the fewer entry points into the lower level exist, limiting the success rate of the initial hierarchical queries, as there are only s/g per merged sub-graph. For $g > s$, some points can only be reached after sub-graphs are bridged by symmetric linking.

To improve the graph quality, refinement steps, as described in Algorithm 6, can be performed which simply repeat the merging and symmetric linking steps throughout the search-graph. While refinement steps would also be beneficial during the actual sub-graph merging, we observed

that performing them in the end is sufficient for the overall quality of the search structure.

Algorithm 6. Parallel Graph Refinement

Function RefineGraph (graph, l_{top}):
Input: search structure graph, top layer l_{top}
Result: refined search structure graph
for $l_m \leftarrow l_{top} - 1$ **to** 0 :
 graph.merge(l_{top} , l_m)
 graph.sym(l_m)

5.4 Query Considerations

For our approach, during graph construction, it is crucial to perform a hierarchical query, which searches nearest neighbors layer by layer, due to the fact that the search index is not yet fully merged. Here, the coarse-to-fine methodology is able to bridge gaps between sub-graphs that are not yet connected and provides multiple routes to the area of interest. Starting from multiple spread-out points increases the quality significantly. In particular, if not only the 1-NN is of importance but also the neighbors at the far end of k . However, for a converged search-graph, this effort is no longer necessary as all points are interlinked well.

Searching in flat index structures does not have the hierarchical overhead. For example, Li *et al.* [21] start their query always from the centroid in a flat graph. Nevertheless, as the number of points grows, the number of hops to the centroid grows as well. In addition, with a single starting point, any goal point will be approached from just one direction. The search might be prone to gaps or linking problems inside the search-graph.

In our design, the bottom layer is actually a flat graph that has all points included. When searching the finished search-graph for nearest neighbors of novel points, it turned out to be more efficient in practice to skip the intermediate layers and continue the search directly on the bottom layer after exploring the s start points that make up the top layer. This allows to significantly cut back on the search iterations performed as otherwise the search would need to iterate on each intermediate layer. In practice, compared with the hierarchical approach, we did not observe any loss in recall but a significant saving in time.

5.5 Multi-GPU

The parallel construction and search algorithm can be extended to multiple GPUs. Johnson *et al.* [2] distinguish between two types of multi-GPU parallelism: *Replication* and *Sharding*. *Replication* copies the entire dataset \mathcal{X} to multiple GPUs to parallelize the query process even further. The queries \mathcal{Q} are divided equally among the available GPUs, resulting in linear speedups.

Sharding subdivides the dataset \mathcal{X} into smaller, independent shards. This allows us to process billion-scale datasets which would otherwise not fit into GPU memory. When necessary, shards can also be swapped into main memory or onto disk. All GPUs construct the search-graphs for their shards in parallel. Since each shard has lower complexity due to the reduced number of points, super-linear speedups *w.r.t.* the same quality can be achieved.

The downside is that all shards need to be processed for each query. When querying multiple shards per GPU, we swap already processed shards for new ones in the background to hide memory latencies. Still, swapping shards puts a limit on the minimum run time per query batch. As some additional overhead, the individual query results per shard need to be merged. Within each GPU, we use a parallel radix sort. The final result across the GPUs is computed on the CPU using an efficient n -way merge.

6 EMPIRICAL EVALUATION

In the following, we evaluate the performance of the proposed approach and its individual components on several publicly available benchmark datasets and report qualitative and quantitative results in terms of timings and accuracy.

Datasets. We ran experiments on datasets of varying sizes and dimensionality generated in different application contexts: SIFT1M [11] and SIFT1B [12] containing SIFT vectors of dimension 128, DEEP1B [5] with 1 billion 96-dimensional feature vectors encoding entire images, NyTimes [35], [36] and GloVe 200 [35], [37], which are two skewed and clustered datasets containing random projections of word embeddings compared using cosine-similarity, and finally the 960-dimensional dataset GIST [11]. Details on the datasets and construction details for our search graphs can be found in Table 4.

Hardware. We use a machine with 8x NVIDIA Tesla V100 and 2x Intel Xeon Gold 5218, where we usually use just a single GPU, except for SIFT1B and DEEP1B, where we use all 8 GPUs. We publish results for additional GPUs in the supplemental.

Performance Metrics. When comparing results to other approaches, one has to carefully look at the employed metric. The query performance is typically measured in recall ($R@k$). For quantization-based methods (e.g., [11]), the recall is understood as the ratio of queries which return the true first nearest neighbor among the first k results

$$R@k = \frac{|\mathcal{N}_q^{gt}(1) \cap \mathcal{N}_q(k)|}{|\mathcal{N}_q^{gt}(1)|}. \quad (5)$$

For methods with exact distance computations – such as graph-based methods – the recall is instead understood as the overlap between the first k results and the first k true nearest neighbors. For disambiguation, we refer to it as consensus ($C@k$)

$$C@k = \frac{|\mathcal{N}_q^{gt}(k) \cap \mathcal{N}_q(k)|}{|\mathcal{N}_q^{gt}(k)|}. \quad (6)$$

As our algorithm uses exact distance calculations, the true nearest neighbor is either reported as the first element in an answer or not found at all. Therefore, we report only $R@1$ ($=C@1$).

Batch Size. The number of queries executed per batch is an important factor for GPU-based queries, which we analyze in Fig. 8b. In our experiments, we measure the time for executing all 10000 queries (except 1000 queries for GIST [11]) in a batch and report the total execution time

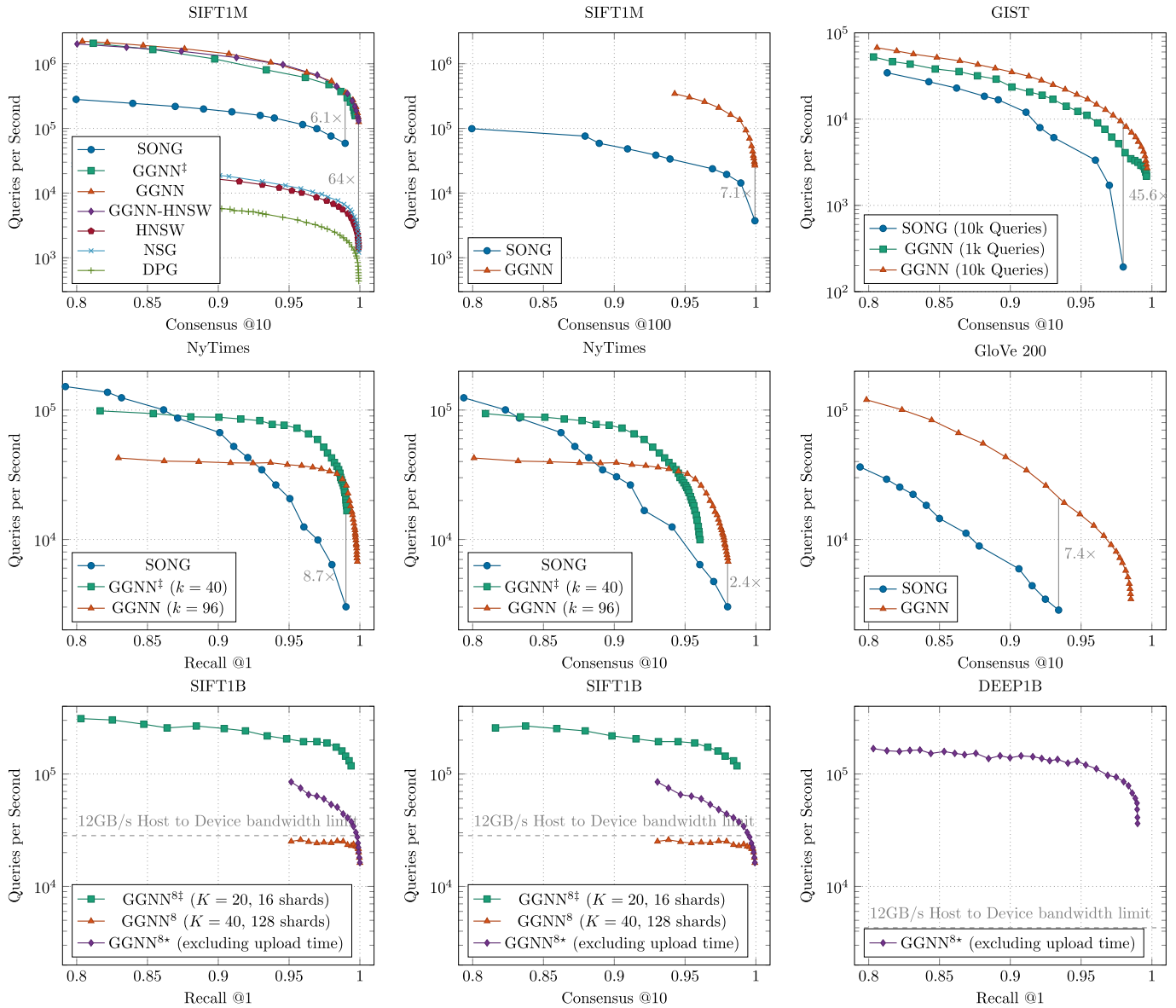


Fig. 5. Performance comparison across various datasets and top- k queries. Results in the top-right corner are preferable. We compare mainly against SONG [3], using the values from their paper and using the same GPU. On SIFT1M, we additionally compare against state-of-the-art single-core CPU-based methods [20], [21], [26] and include a configuration “GGNN-HNSW”, where we use our method to query the graph built by HNSW [20], like SONG [3] does. Our query significantly outperforms SONG and achieves similar results as a query on a similarly-sized search-graph constructed in much less time using our method. High performance is also achieved when querying for the 100 nearest neighbors or more complicated datasets like GloVe 200 or very high dimensional datasets like GIST. On the rather small NyTimes dataset, our graph construction appears to be non-optimal but the highly efficient query still manages to outperform SONG by a large factor. Using 8 GPUs, even billion-scale datasets like SIFT1B or DEEP1B can be queried at rates around 100k queries per second with near-perfect recalls.

divided by the number of queries as $\mu\text{s}/\text{query}$ or plot it as queries per second.

6.1 Performance Comparisons

Evaluation is performed on the default configuration GGNN, a faster, less accurate configuration GGNN[‡], and a 8-GPU configuration GGNN⁸ (see Table 4 for parameters).

As reference, we use several recent CPU-based methods [20], [21], [26], where we executed the single-threaded reference implementations on an Intel Core i7-9700K. We further compare against the GPU-based SONG [3] and mimic their approach of querying the bottom layer of a prebuilt HNSW [20] graph using our query as “GGNN-HNSW”. Using our query is even faster. In addition, it performs very

similar to querying a similarly sized graph constructed using our method in significantly less time. Detailed performance comparisons are shown in Fig. 5 and Tables 1, 2, and 3. In the tables, we compare against previously published results, where GPU-based methods [1], [2], [8], [18] used NVIDIA GTX Titan X GPUs, and [9] used an Arria 10 GX1150 FPGA. Besides being significantly faster on all datasets (around $1\mu\text{s}$ per query on SIFT1M), our method can also achieve very high recall rates, close to perfect.

6.2 Search-Graph Construction

In the following, we inspect several aspects of the construction process, including the time spent on the individual construction steps, the influence of the dataset size, the

TABLE 1
Million-Scale Performance Comparison

Approach	τ_q	SIFT1M [11]			
		Query time $\mu\text{s}/\text{query} \downarrow$	Recall @1 \uparrow	Recall @10 \uparrow	Recall @100 \uparrow
LOPQ [13]		51100	0.51	0.93	0.97
IVFPQ [11]		11200	0.28	0.70	0.93
FLANN [10]		5320	0.97	-	-
HM-ANN [27]		855	0.9995	-	-
<hr/>					
PQT [1]		236	0.99	-	-
FAISS [2]		20	0.51	0.83	0.86
PQFPGA [9]		20	0.80	0.88	0.95
FANNG [8]		20	0.88	0.94	0.97
<hr/>					
GGNN	0.65	5.8	0.9997	-	-
	0.42	1.5	0.99	-	-
	0.30	0.7	0.95	-	-
	0.20	0.5	0.90	-	-
<hr/>					
Brute Force (1x V100)		381.4	1.0	-	-

TABLE 2
Performance Comparison on SIFT1B [12]

Approach	τ_q	SIFT1B [12]			
		Query time $\mu\text{s}/\text{query} \downarrow$	Recall @1 \uparrow	Recall @10 \uparrow	Recall @100 \uparrow
LOPQ [13]		8000	-	0.20	-
IVFPQ [11]		74000	0.08	0.37	0.73
Multi-D-ADC [15]		1603	0.33	0.80	0.98
HM-ANN [27]		1014	0.99	-	-
PQT [1]		150	0.14	0.35	0.57
FAISS [2]		17.7	-	0.37	-
PQFPGA [9]		20	-	0.55	-
RobustIQ [18]		33	0.33	0.76	0.90
<hr/>					
GGNN ⁸	0.56	61.6	1.0	-	-
	0.50	46.4	0.999	-	-
	0.38	42.7	0.99	-	-
<hr/>					
GGNN ^{8†}	0.61	7.1	0.99	-	-
	0.42	3.9	0.90	-	-
<hr/>					
Brute Force (8x V100)		≈ 30000	1.0	-	-

Our method GGNN⁸ used 8 GPUs. RobustIQ [18] used 2 GPUs. Otherwise, single CPUs or GPUs were used. Our method achieves perfect recall@1. GGNN⁸ is limited by the host to device memory bandwidth and could otherwise perform the query with 99% recall@1 in just 24.5 $\mu\text{s}/\text{query}$ (see Section 6.3.1). The smaller GGNN^{8†} can be queried much faster, since it iterates over fewer shards and fits on the GPUs in one piece.

resulting graph quality in terms of nearest neighbors per point, and how additional construction time can be traded in for even faster queries.

6.2.1 Construction Time

Construction times and index sizes of our method are listed in Table 4. For comparison, FAISS [2] report construction times between 4 and 24 hours for DEEP1B, yet reaches less than 50% R@1. HM-ANN [27] report construction times around 100 hours for effective billion-scale search-graphs. Using our hierarchical GPU-based graph-merge algorithm, 99% R@1 on

TABLE 3
Performance Comparison on DEEP1B [5]

Approach	τ_q	DEEP1B [5]			
		Query time $\mu\text{s}/\text{query} \downarrow$	Recall @1 \uparrow	Recall @10 \uparrow	Recall @100 \uparrow
Multi-D-ADC [15]		1065	0.37	0.74	0.92
HM-ANN [27]		1142	0.99	-	-
FAISS [2]		13.3	0.45	-	-
RobustIQ [18]		30	0.38	0.75	0.89
<hr/>					
GGNN ^{8*}	1.50	27.6	0.99	-	-
	0.44	8.3	0.95	-	-
	0.36	7.2	0.90	-	-

Our method GGNN⁸ used 8 GPUs. FAISS [2] used 4 GPUs. RobustIQ [18] used 2 GPUs. Otherwise, single CPUs were used. GGNN⁸ is limited by the host to device memory bandwidth to at least 233 $\mu\text{s}/\text{query}$ on the 10k queries set (see Section 6.3.1). To show the influence of τ_q and to compare with future hardware configurations, we report times without the currently necessary upload as GGNN^{8*}.

DEEP1B and even perfect 100% R@1 SIFT1B can be reached with fast queries while the construction takes less than 2 hours.

6.2.2 Construction Time Composition

Fig. 6 shows the time spent on the individual graph-construction operations with 2 refinement iterations. The majority of the construction time is spent on the merge operation, especially those merges which involve the bottom layer, where the merge operation searches for the k nearest neighbors for all points in the dataset.

6.2.3 Dataset Size

Efficient graph construction needs to scale well with the size of the dataset. As demonstrated in Fig. 7, the construction time scales almost linearly with the size of the dataset, $\approx O(n^{1.077})$. This can be explained by most of the construction time being spent on independently determining the neighbors of each bottom-level point (see Section 6.2.2). This almost linear behavior is significantly better than the complexity of brute-force kNN construction $O(n^2)$.

6.2.4 For-All Queries

The fast construction of the kNN search graph from scratch solves another interesting problem on the side, namely computing the k nearest neighbors for all points in the dataset, as frequently encountered in n-body problems. When we construct the full hierarchy, the final merging step effectively searches for the k neighbors of all points. In Table 5, we demonstrate the quality of the for-all problem considering the consensus. Referring to Fig. 7, this for-all problem again shows almost a linear behavior. In case of sharding, though, all points would need to be tested once against every shard. As the number of shards linearly depends on the number of points one approaches $O(n^2)$ complexity again with a tiny constant though, e.g., 16 shards for the SIFT1B dataset.

6.2.5 The Construction-Query Trade-Off

Our graph construction algorithm and the query can be tuned for speed or accuracy. The build time is controlled by the slack factor τ_b and by how many refinement iterations r are carried

TABLE 4
Datasets and Search Graph Construction Details

Dataset			Search Graph Configuration						Construction Time and Graph Size			
Dataset	#Points	#Dim.	Config.	k	s	l	τ_b	r	GPU	Time	Size	
SIFT1M [11]	1 000 000	128	GGNN [‡]	24	32	4	0.5	2	1x V100	9.2 s	95 MiB	
			GGNN	40	32	4	0.5	2		21.8 s	158 MiB	
NyTimes [35], [36]	290 000	256	GGNN [‡]	40	32	4	0.3	0		13.4 s	46 MiB	
			GGNN	96	64	4	0.3	0		39.3 s	113 MiB	
GloVe 200 [35], [37]	1 183 514	200	GGNN	96	64	4	0.5	2		6.0 min	450 MiB	
GIST [11]	1 000 000	960	GGNN	96	64	4	0.4	2		11.9 min	382 MiB	
SIFT1B [12]	1 000 000 000	128	GGNN ^{8‡}	20	32	4	0.5	2	8x V100	16 shards	33.4 min	75 GiB
			GGNN ⁸	40	32	4	0.5	2		128 shards	78.6 min	152 GiB
DEEP1B [5]	1 000 000 000	96	GGNN ⁸	24	32	4	0.5	2	32 shards	47.5 min	90 GiB	

For some datasets, we also demonstrate the construction-query trade-off with a faster construction version ([‡]). All configurations shown here are capable of reaching at least 99% recall@1.

out. The longer the construction time, the more precise the resulting graph. A quickly assembled graph will have worse edges and a query might need to visit more nodes until fulfilling the stopping criterion. In Fig. 8a, the trade-off between build time and query time is visualized for fixed recall rates.

6.3 Query Behaviour

The runtime and the quality of a query can be controlled by adapting the stopping criterion through the slack factor τ_q . As can be seen e.g., in Table 1, by increasing τ_q , a larger safety margin is considered during query, resulting in better recall rates at the cost of visiting more points and consequently longer query time.

It is instructive to look at the behaviour of the query over time. In Fig. 9, the initial distance of the query to the starting point, i.e., the closest point on the top layer, is drastically reduced already after very few iterations. Here, an iteration stands for fetching the best point from the priority queue

and calculating the distance to all its neighbors. Most time is spent to carefully explore the neighborhood around the true nearest neighbor. Quickly after locating the best candidates, the query is terminated by the stopping criterion to prevent unnecessary iterations. This effect does not only show up in the small subset of plotted query distances, but also statistically in the histogram over all queries.

6.3.1 Out of GPU-Memory Queries

When querying on billion-scale datasets, the amount of necessary GPU-memory will quickly exceed the available memory even on an 8 NVIDIA Tesla V100 system. While SIFT1B together with the low-profile graph GGNN^{8‡} still fits on the GPUs, with the GGNN⁸ graph, it exceeds the available

TABLE 5
Accuracy of the Nearest Neighbors for Each Point in the Dataset, as Contained Within Our Search Graph

Method	Dataset	C@1 \uparrow	C@10 \uparrow
GGNN [‡]	SIFT1M	0.996	0.981
GGNN		0.999	0.998

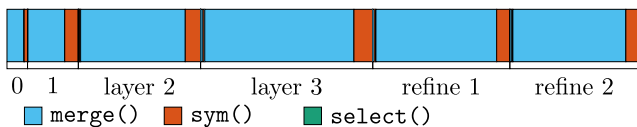


Fig. 6. Split-up of the construction time for the SIFT1M search graph. Most time is spent on the merge operation (86.92%), some time on the sym operation (13.06%) and almost no time on selecting the points for the upper layers (0.02%).

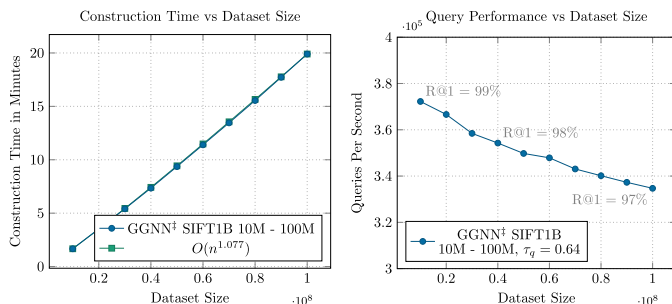


Fig. 7. Construction times and queries per second for increasing subsets of SIFT1B (up to 100M) on a single GPU. The construction time almost linearly depends on the dataset size. With increasing dataset size, the query performance suffers slightly in both execution time and accuracy for a constant slack factor τ_q .

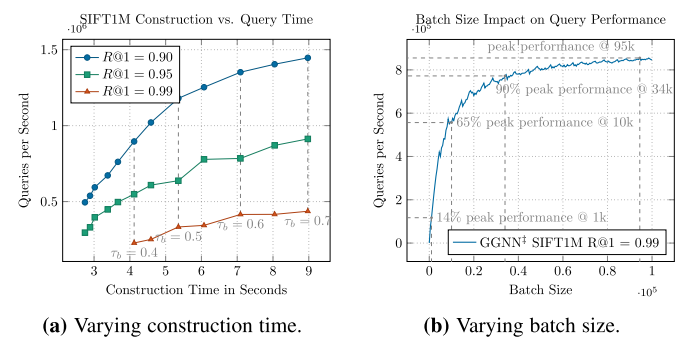
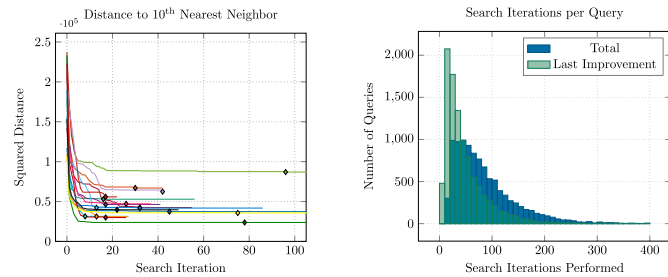


Fig. 8. Query performance depends both on the quality of the search graph and the number of queries executed simultaneously. Queries with the same accuracy can be executed faster if more time is spent on construction (a). Here, no refinement is performed ($r = 0$) to visualize the influence of τ_b on the initial construction. Generally, having a few refinement iterations can further boost query performance. In terms of query size (b), high performance is already reached for a few thousand queries, while further simultaneous queries yield even better performance with a peak at 95k queries.



(a) Development of the 10th best query point as the query progresses. (b) Iterations performed total, and until the last improvement is found.

Fig. 9. Looking at the behavior of several queries (a), one can see that the general area is found very quickly by the search graph. Afterwards, the local neighborhood is explored and shortly after finding the last improvement (indicated by the marker), the query is terminated by the stopping criterion. The effectiveness of the stopping criterion also shows in the statistics (b). The distribution of total iterations closely follows the distribution of iterations necessary to make the final improvement, only lagging behind by a handful of iterations.

memory by 2 shards (4.2 GiB). On DEEP1B, the dataset alone already surpasses the available memory, and with GGNN⁸ an additional 28 GiB per GPU need to be loaded per query pass. This results in a bound that is defined by the host to device memory throughput (≈ 12 GiB/s [38]), i.e., for 10k queries, this results in a minimum of $35\mu\text{s}/\text{query}$ on SIFT1B and $233\mu\text{s}/\text{query}$ on DEEP1B. These bounds are shown in Fig. 5. Note that this loading time can be hidden completely by performing an overall costlier query, e.g., using more queries, increased τ_q , or larger caches. For easy comparison with future approaches on devices with sufficient memory, we also report the computation time without the memory transfers.

7 CONCLUSION

Our proposed parallel GPU-based search algorithm is surpassing all state-of-the-art algorithms in terms of speed by a large factor and represents the fastest ANN query technique while maintaining recall rates above 99%. The efficient query algorithm further accelerates the parallel construction and merging of sub-graphs. Our hierarchical construction scheme creates high-quality kNN graphs with graph-diversification links for very efficient traversal. It is easily deployed in multi-GPU systems to cope with very large-scale datasets. It is the first ANN search method capable of constructing effective search structures ($R@1 \geq 0.99$) for billion-scale datasets in less than an hour. For million-scale datasets, search-graphs of sufficient quality can often be constructed within seconds, allowing for quick nearest-neighbor searches also on intermediate data structures as a part of larger GPU-based algorithms, e.g., in machine learning applications.

Currently, our method computes the exact distance to all visited high-dimensional points. As the number of distance calculations dominates the query time, a compressed representation of the data vectors could lead to further acceleration.

ACKNOWLEDGMENTS

Fabian Groh and Patrick Wieschollek completed this work prior to joining Amazon. During the work of this paper, all authors were member of the Computer Graphics Group at the University of Tübingen.

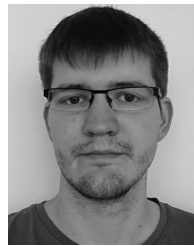
REFERENCES

- [1] P. Wieschollek, O. Wang, A. Sorkine-Hornung, and H. P. A. Lensch, "Efficient large-scale approximate nearest neighbor search on the GPU," in *Proc. IEEE Conf. Comput. Vis. Pattern Recognit.*, 2016, pp. 2027–2035.
- [2] J. Johnson, M. Douze, and H. Jégou, "Billion-scale similarity search with GPUs," *IEEE Trans. Big Data*, vol. 7, no. 3, pp. 535–547, Jul. 2021.
- [3] W. Zhao, S. Tan, and P. Li, "SONG: Approximate nearest neighbor search on GPU," in *Proc. IEEE 36th Int. Conf. Data Eng.*, 2020, pp. 1033–1044.
- [4] R. Weber, H.-J. Schek, and S. Blott, "A quantitative analysis and performance study for similarity-search methods in high-dimensional spaces," in *Proc. 24th Int. Conf. Very Large Data Bases*, 1998, pp. 194–205.
- [5] A. B. Yandex and V. Lempitsky, "Efficient indexing of billion-scale datasets of deep descriptors," in *Proc. IEEE Conf. Comput. Vis. Pattern Recognit.*, 2016, pp. 2055–2063.
- [6] J. Bobadilla, F. Ortega, A. Hernando, and A. Gutiérrez, "Recommender systems survey," *Knowl.-Based Syst.*, vol. 46, pp. 109–132, 2013.
- [7] W. Chen *et al.*, "Vector and line quantization for billion-scale similarity search on GPUs," *Future Gener. Comput. Syst.*, vol. 99, pp. 295–307, Oct. 2019.
- [8] B. Harwood and T. Drummond, "FANNG: Fast approximate nearest neighbour graphs," in *Proc. IEEE Conf. Comput. Vis. Pattern Recognit.*, 2016, pp. 5713–5722.
- [9] J. Zhang, S. Khoram, and J. Li, "Efficient large-scale approximate nearest neighbor search on OpenCL FPGA," in *Proc. IEEE Conf. Comput. Vis. Pattern Recognit.*, 2018, pp. 4924–4932.
- [10] M. Muja and D. G. Lowe, "Scalable nearest neighbor algorithms for high dimensional data," *IEEE Trans. Pattern Anal. Mach. Intell.*, vol. 36, no. 11, pp. 2227–2240, Nov. 2014.
- [11] H. Jégou, M. Douze, and C. Schmid, "Product quantization for nearest neighbor search," *IEEE Trans. Pattern Anal. Mach. Intell.*, vol. 33, no. 1, pp. 117–128, Jan. 2011.
- [12] H. Jégou, R. Tavenard, M. Douze, and L. Amsaleg, "Searching in one billion vectors: Re-rank with source coding," in *Proc. IEEE Int. Conf. Acoust. Speech Signal Process.*, 2011, pp. 861–864.
- [13] Y. Kalantidis and Y. Avrithis, "Locally optimized product quantization for approximate nearest neighbor search," in *Proc. IEEE Conf. Comput. Vis. Pattern Recognit.*, 2014, pp. 2329–2336.
- [14] T. Ge, K. He, Q. Ke, and J. Sun, "Optimized product quantization for approximate nearest neighbor search," in *Proc. IEEE Conf. Comput. Vis. Pattern Recognit.*, 2013, pp. 2946–2953.
- [15] A. Babenko and V. Lempitsky, "The inverted multi-index," in *Proc. IEEE Conf. Comput. Vis. Pattern Recognit.*, 2012, pp. 3069–3076.
- [16] A. Babenko and V. Lempitsky, "Tree quantization for large-scale similarity search and classification," in *Proc. IEEE Conf. Comput. Vis. Pattern Recognit.*, 2015, pp. 4240–4248.
- [17] A. Babenko and V. Lempitsky, "Additive quantization for extreme vector compression," in *Proc. IEEE Conf. Comput. Vis. Pattern Recognit.*, 2014, pp. 931–938.
- [18] W. Chen, J. Chen, F. Zou, Y.-F. Li, P. Lu, and W. Zhao, "RobustQ: A robust ANN search method for billion-scale similarity search on GPUs," in *Proc. Int. Conf. Multimedia Retrieval*, 2019, pp. 132–140.
- [19] Y. Matsui, T. Yamasaki, and K. Aizawa, "PQTable: Fast exact asymmetric distance neighbor search for product quantization using hash tables," in *Proc. IEEE Int. Conf. Comput. Vis.*, 2015, pp. 1940–1948.
- [20] Y. A. Malkov and D. A. Yashunin, "Efficient and robust approximate nearest neighbor search using hierarchical navigable small world graphs," *IEEE Trans. Pattern Anal. Mach. Intell.*, vol. 42, no. 4, pp. 824–836, Apr. 2020.
- [21] W. Li *et al.*, "Approximate nearest neighbor search on high dimensional data-experiments, analyses, and improvement," *IEEE Trans. Knowl. Data Eng.*, vol. 32, no. 8, pp. 1475–1488, Aug. 2020.
- [22] W. Dong, C. Moses, and K. Li, "Efficient K-nearest neighbor graph construction for generic similarity measures," in *Proc. 20th Int. Conf. World Wide Web*, 2011, pp. 577–586.
- [23] J. Chen, H.-R. Fang, and Y. Saad, "Fast approximate kNN graph construction for high dimensional data via recursive Lanczos bisection," *J. Mach. Learn. Res.*, vol. 10, no. Sep., pp. 1989–2012, 2009.
- [24] T. Warashina, K. Aoyama, H. Sawada, and T. Hattori, "Efficient K-nearest neighbor graph construction using MapReduce for large-scale data sets," *IEICE Trans.*, vol. 97-D, pp. 3142–3154, 2014.

- [25] C. Fu and D. Cai, "EFANNA: An extremely fast approximate nearest neighbor search algorithm based on kNN graph," 2016, *arXiv:1609.07228*.
- [26] C. Fu, C. Xiang, C. Wang, and D. Cai, "Fast approximate nearest neighbor search with the navigating spreading-out graph," *Proc. VLDB Endowment*, vol. 12, no. 5, pp. 461–474, 2019.
- [27] J. Ren, M. Zhang, and D. Li, "HM-ANN: Efficient billion-point nearest neighbor search on heterogeneous memory," in *Proc. 34th Conf. Neural Inf. Process. Syst.*, vol. 33, 2020, pp. 10672–10684.
- [28] J. H. Friedman, J. L. Bentley, and R. A. Finkel, "An algorithm for finding best matches in logarithmic expected time," *ACM Trans. Math. Softw.*, vol. 3, no. 3, pp. 209–226, Sep. 1977.
- [29] M. Datar, N. Immorlica, P. Indyk, and V. S. Mirrokni, "Locality-sensitive hashing scheme based on p-stable distributions," in *Proc. 20th Annu. Symp. Comput. Geometry*, 2004, pp. 253–262.
- [30] A. Andoni and P. Indyk, "Near-optimal hashing algorithms for approximate nearest neighbor in high dimensions," *Commun. ACM*, vol. 51, no. 1, Jan. 2008, Art. no. 117.
- [31] S. Korman and S. Avidan, "Coherency sensitive hashing," in *Proc. IEEE Int. Conf. Comput. Vis.*, 2011, pp. 1607–1614.
- [32] D. S. Kim and N. B. Shroff, "Quantization based on a novel sample-adaptive product quantizer (SAPQ)," *IEEE Trans. Inf. Theory*, vol. 45, no. 7, pp. 2306–2320, Nov. 1999.
- [33] Y. Linde, A. Buzo, and R. Gray, "An algorithm for vector quantizer design," *IEEE Trans. Commun.*, vol. 28, no. 1, pp. 84–95, Jan. 1980.
- [34] P. S. Efraimidis and P. G. Spirakis, "Weighted random sampling with a reservoir," *Inf. Process. Lett.*, vol. 97, no. 5, pp. 181–185, 2006.
- [35] M. Aumüller, E. Bernhardsson, and A. Faithfull, "ANN-benchmarks: A benchmarking tool for approximate nearest neighbor algorithms," *Inf. Syst.*, vol. 87, 2020, doi: [10.1016/j.is.2019.02.006](https://doi.org/10.1016/j.is.2019.02.006).
- [36] D. Dua and C. Graff, "UCI machine learning repository," 2017. Accessed: Dec. 01, 2020. [Online]. Available: <http://archive.ics.uci.edu/ml>
- [37] J. Pennington, R. Socher, and C. D. Manning, "GloVe: Global vectors for word representation," in *Proc. Conf. Empir. Methods Nat. Lang. Process.*, 2014, pp. 1532–1543.
- [38] Z. Jia, M. Maggioni, B. Staiger, and D. P. Scarpazza, "Dissecting the NVIDIA volta GPU architecture via microbenchmarking," 2018, *arXiv:1804.06826*.



Fabian Groh received the diploma in computer science from Ulm University, Ulm, Germany, in 2013. He is currently working toward the PhD degree in the Computer Graphics Group, University of Tübingen, Tübingen, Germany. His primary research topics are processing and learning on unstructured data in large-scale settings by utilizing GPU-based designs. In 2020, he joined Amazon Tübingen.



Lukas Ruppert received the master of science degree in computer science from the University of Tübingen, Tübingen, Germany, in 2019. He is currently working toward the PhD degree in computer graphics with a focus on physically based rendering.



Patrick Wieschollek received the master of science degree from Friedrich-Schiller University, Germany, Jena, Germany, in 2014. He wrote his PhD thesis at the Computer Graphics Group, University of Tübingen, Tübingen, Germany and Max Planck Institute for Intelligent Systems in Tübingen, Tübingen, Germany. His primary research topic is developing data-driven approaches for multi-frame and unstructured data in large-scale settings. In 2019, he joined Amazon Tübingen.



Hendrik P. A. Lensch received the diploma in computers science from the University of Erlangen, Erlangen, Germany, in 1999, and the PhD degree from Saarland University, Saarbrücken, Germany, in 2003. He holds the chair for computer graphics with Tübingen University. He worked as a research associate with the Computer Graphics Group, Max-Planck-Institut für Informatik in Saarbrücken, Germany. He spent two years (2004–2006) as a visiting assistant professor with Stanford University, USA. From 2009 to 2011, he was a full professor with the Institute for Media Informatics, Ulm University, Germany. In his career, he received the Eurographics Young Researcher Award 2005 and was awarded an Emmy Noether Fellowship by the German Research Foundation (DFG) in 2007. His research interests include 3D appearance acquisition, computational photography, machine learning, global illumination and image-based rendering, and massively parallel programming.

▷ **For more information on this or any other computing topic, please visit our Digital Library at www.computer.org/csdl.**